Crystal Structures of the α and β Forms of K$_2$ZnGeO$_4$

C. Colbeau-Justin,[1] G. Wallez, A. Elfakir, and M. Quarton

Laboratoire de Cristallochimie du Solide, CNRS-URA 1388, Université P. et M. Curie, 4 place Jussieu, 75252 Paris Cedex 05, France

and

E. Suard

Institut Laue Langevin, Rue des Martyrs, BP 156, 38042 Grenoble Cedex, France

The crystal structures of two phases of K$_2$ZnGeO$_4$ have been refined by the Rietveld method using neutron powder diffraction data, at 298 K (α form) and 1153 K (β form), to $R_B = 4.8$ and 7.3%, respectively. α-K$_2$ZnGeO$_4$ is orthorhombic, $a = 11.1131(4)$ Å, $b = 5.5369(2)$ Å, $c = 15.8629(5)$ Å, space group $Pca2_1$, and $Z = 8$. β-K$_2$ZnGeO$_4$ is cubic, $a = 8.0254(5)$ Å, space group $F\bar{4}3m$, and $Z = 4$. Phase transition between α and β forms occurs at 1049 K. Both phases are stuffed cristobalites and correspond to a distortion of the ideal cristobalite structure. Neutron diffraction data show an ordered and alternating arrangement of ZnO$_4$ and GeO$_4$ tetrahedra in α-K$_2$ZnGeO$_4$. The β phase shows a static or dynamic superposition of short-range ordered clusters analogous to SiO$_2$ cristobalite. © 1997 Academic Press

INTRODUCTION

The present study concerns investigations on new oxide compounds carried out to establish the correlations between structure and ferroelectric properties. A ferroelectric compound shows spontaneous polarization. Specific conditions are required for the existence of ferroelectricity: the point group must be polar and the spontaneous polarization must be reversible under electrostatic strain. Furthermore, structures have to be flexible enough to allow transition from one stable ferroelectric state to the other. For this reason, we focused our research on distortions induced by the differentiation of the tetrahedra in SiO$_2$-related frameworks or by the insertion of a large monovalent cation in the cavities of these structures. The study of K$_2$ZnGeO$_4$ is part of a program dealing with the stuffed cristobalite structure-type compounds of general formula

$A_2^I B^{II} X^{IV} O_4$ (A^I = K, Rb, Cs; B^{II} = Zn, Mg, Cd; X^{IV} = Si, Ge, Ti) (1–4).

Differential thermal analysis of K$_2$ZnGeO$_4$ (1) from room temperature to 1673 K shows that a reversible phase transition occurs at 1049 K and the melting point at 1573 K. Low-temperature X-ray diffraction data did not allow detection of any other phase transition in the range from 120 K to room temperature. By analogy with SiO$_2$ cristobalite, the phase will be referenced as the α form below and as the β form above the transition.

X-ray powder diffraction data had already been used to study α-K$_2$ZnGeO$_4$ (5), but an average structure was obtained because ZnO$_4$ and GeO$_4$ tetrahedra were considered equivalent to reduce the number of parameters to refine. Furthermore, the very similar X-ray scattering factors of Zn and Ge atoms do not allow them to be distinguished, so the distribution of ZnO$_4$ and GeO$_4$ tetrahedra remains undetermined. A statistical distribution implies space group $Pcab$ (centric), whereas an ordered and alternating arrangement leads to the $Pca2_1$ (acentric) space group, and the presence of a symmetry center is fatal to the ferroelectricity.

We synthesized K$_2$ZnGeO$_4$ and recorded neutron powder diffraction patterns to fully determine its α-form structure and to answer the question linked to the existence of a symmetry center. Furthermore, because knowledge of each stable phase of K$_2$ZnGeO$_4$ is needed to characterize the ferroelectric properties (potential ferroelectric transitions), we made neutron powder diffraction experiments at 1153 K to determine the structure of β-K$_2$ZnGeO$_4$.

PREPARATION AND MEASUREMENTS

K$_2$ZnGeO$_4$ was synthesized by solid-state reaction in air according to the chemical reaction:

$$K_2CO_3 + ZnO + GeO_2 \xrightarrow{1073\,K} K_2ZnGeO_4 + CO_2.$$

[1] To whom correspondence should be addressed. Present address: Laboratoire d'Ingénierie des Matériause et des Hautes Pressions, Université Paris, Nord, Avenue J. B. Clément, 93430 Villetaneuse, France.
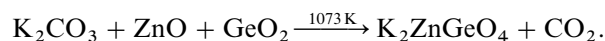
TABLE 1
Data Collection

Radiation	Neutrons	
Instrument	D2B (ILL)	
Wavelength	1.5938(2) Å	
Temperature	298 K	1153 K
Sample holder	Vanadium airtight capsule	Quartz tube
Particle size	$\approx 10 \ \mu m$	
2θ range	8.0–158.8°	
Step	0.05° (2θ)	
Monitor	15,000	

FIG. 1. Observed and calculated neutron powder diffraction patterns and difference plot of α-K_2ZnGeO_4.

Stoichiometric amounts of dried reactants were thoroughly blended, placed in a platinum crucible, and submitted to heat treatments in air at 473 K for 6 h (loss of carbon dioxide) and at 1073 K for 24 h after homogenization by grinding. This synthesis procedure leads to a pure compound unlike the previously published one (5).

Powder neutron diffraction data were collected on the D2B diffractometer of the Institut Laue-Langevin (Grenoble, France) at 298 and 1153 K. The high resolution powder diffractometer D2B has a bank of 64 detectors spaced at 2.5 degrees intervals. A monochromatic incident beam is obtained by reflection on (335) planes of a germanium single crystal. Experimental data are summarized in Table 1.

STRUCTURAL REFINEMENTS

The structures of α-K_2ZnGeO_4 and β-K_2ZnGeO_4 have been determined by Rietveld refinements of neutron powder diffraction data. The structures were refined using the Fullprof program (6). A pseudo-Voigt function was used to model the peak shape.

α-K_2ZnGeO_4

Starting atomic parameters were taken from the previously published average K_2ZnGeO_4 structure (5). Refinements in space group $Pcab$ were not satisfactory (R_B = 20%), so the $Pca2_1$ space group has been used. The background was described by a third-order polynomial function of 2θ. Fifty-four structural and six profile parameters were varied during the last computation.

The observed and calculated neutron diffraction patterns and a difference plot are shown in Fig. 1. Agreement factors (R values) are listed in Table 2. Cell data of α-K_2ZnGeO_4 are reported in Table 3. The cell parameters given originate from the Rietveld refinement. Final atomic coordinates and Debye–Waller parameters are listed in Table 4, and coordination polyhedra and bond angles in Table 5.
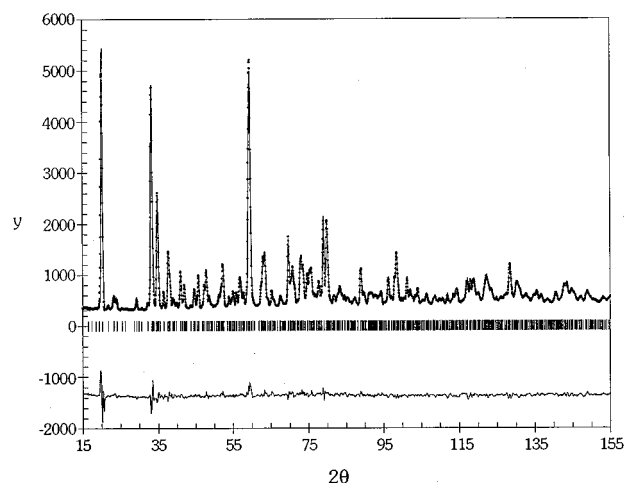
β-K_2ZnGeO_4

The neutron powder pattern of β-K_2ZnGeO_4 was indexed on the basis of a face-centered cubic unit cell. So, starting atomic parameters were taken from the ideal form of K_2ZnGeO_4 (space group $F\overline{4}3m$, see detailed description in next section). In this case, the oxygen atom is on the Zn–Ge line (16e Wyckoff position) leading to a Zn–O–Ge angle of 180°. This refinement leads to too high values of the reliability factors (R_B = 25%), abnormally short Zn–O and Ge–O bonds (1.86 and 1.59 Å instead of 1.95 and 1.77 Å in α-K_2ZnGeO_4), and an excessively high Debye–Waller parameter for oxygen (17 Å^2). Therefore, we moved the oxygen atom from the Zn–Ge line and refined its three atomic coordinates on the basis of a 96i Wyckoff position. The high multiplicity of this position imposes a 1/6 occupancy for oxygen atom to respect the stoichiometry of the compound.

The background was determined by linear interpolation between some points of the experimental pattern; the strong diffuse scattering from the quartz tube did not allow refinement of a polynomial background. Eight structural and six profile parameters were varied in the final refinement.

TABLE 2
Refinement Details for α-K_2ZnGeO_4

Number of refined parameters	66
Independent reflections	997
R_p	3.78%
R_{wp}	5.38%
R_{exp}	1.76%
R_B	4.79%
R_F	2.67%
χ^2	9.36

TABLE 3
Crystal Data for α-K$_2$ZnGeO$_4$

Space group	$Pca2_1$
Z	8
F.W.	280.16 g·mol^{-1}
a	11.1131(4) Å
b	5.5369(2) Å
c	15.8629(5) Å
V	976.1(2) Å^3
d_{calc}	3.81 g·cm^{-3}

The observed and calculated neutron diffraction patterns and a difference plot are shown in Fig. 2. Corresponding agreement R factors are given in Table 6. Cell data for β-K$_2$ZnGeO$_4$ are reported in Table 7. The final atomic coordinates and Debye–Waller parameters are listed in Table 8.

DESCRIPTION OF THE STRUCTURES

The two forms of K$_2$ZnGeO$_4$ can be related to the cristobalite variety of SiO$_2$ (C9 structure) originally proposed by Wyckoff (7). As this structure is now known to be only an approximation of the real structure, it is qualified as an "ideal cristobalite form" corresponding to the diamond packing of SiO$_4$ tetrahedra. In this case, tetrahedral and octahedral diamond interstices are transformed in one kind of 12-coordinated cavity. In ideal K$_2$ZnGeO$_4$, SiO$_4$ tetrahedra are alternatively substituted by ZnO$_4$ and GeO$_4$ tetrahedra. K$^+$ cations occupy the previously mentioned 12-coordinated cavities. Ideal K$_2$ZnGeO$_4$ is cubic (space

TABLE 4
Positional and Debye–Waller Parameters for α-K$_2$ZnGeO$_4$

Atom	x/a	y/b	z/c	B (Å^2)
Zn(1)	0.2366(12)	0.0246(20)	0.7543(10)	0.6(2)
Zn(2)	0.0105(12)	0.5039(17)	0	0.6(2)
Ge(1)	0.0082(7)	0.0169(10)	0.1225(9)	0.10(8)
Ge(2)	0.2356(7)	0.5374(12)	0.3795(9)	0.10(8)
K(1)	0.0222(15)	0.5167(28)	0.2467(13)	0.88(9)
K(2)	0.0091(14)	1.0044(33)	0.8736(16)	0.88(9)
K(3)	0.2301(17)	0.5464(29)	0.6309(15)	0.88(9)
K(4)	0.2407(15)	0.0586(32)	0.4941(13)	0.88(9)
O(1)	0.1610(10)	0.0656(18)	0.1493(11)	1.10(5)
O(2)	0.1702(10)	0.5882(17)	0.9669(12)	1.10(5)
O(3)	0.2016(11)	0.3379(18)	0.8041(11)	1.10(5)
O(4)	0.1961(11)	0.8066(16)	0.3319(11)	1.10(5)
O(5)	0.0877(11)	0.8947(19)	0.7075(11)	1.10(5)
O(6)	0.0926(11)	0.4116(19)	0.4089(11)	1.10(5)
O(7)	0.0272(10)	0.8316(18)	0.5320(12)	1.10(5)
O(8)	0.0139(10)	0.3038(16)	0.6033(11)	1.10(5)

group $F\bar{4}3m$), K atoms occupying 4b and 4d positions and Zn, Ge, and O 4c, 4a, and 16e positions, respectively.

α-K$_2$ZnGeO$_4$

α-K$_2$ZnGeO$_4$ crystallizes in the orthorhombic system ($Pca2_1$) and its structure corresponds to a distortion of the C9 pattern. The distortion is due to tilts of tetrahedra leading to a reduction of symmetry.

The orthorhombic cell is obtained from the cubic C9 cell by the following transformation matrix:

$$\begin{bmatrix} 1 & 1 & 0 \\ -\frac{1}{2} & \frac{1}{2} & 0 \\ 0 & 0 & 2 \end{bmatrix}.$$

Figure 3 shows the K$_2$ZnGeO$_4$ double cell in the cubic system of ideal (a) and distorted (b) forms displaying the tetrahedra disorientation.

The framework distortions in cristobalite-type compounds have been modeled by O'Keeffe and Hyde (8) considering rigid tetrahedra rotations. This model is based on the fact that, since the tetrahedra are corner connected, rotation of one imposes restraints on possible rotations of its four neighbors. Considering rotation of one tetrahedron (T) along one axis (arbitrarily chosen as [001]), O'Keeffe and Hyde have described three patterns of rotations corresponding to the possible rotations of the four neighbors (N_x). The pattern I, the simplest one, corresponds to a rotation of all tetrahedra along only one axis: clockwise rotation of T along [001] leads to counterclockwise rotations along the same axis of the four neighbors. With two (noncollinear) rotation axes, the situation is more complicated and O'Keeffe and Hyde have considered only patterns with periodicities no greater than that of the C9 unit cell. The rotation of T along [001] leads to rotations along [010] of the four neighbors in pattern II and to a rotation along [001] of N_1 and N_3 and along [010] of N_2 and N_4 in pattern III.

Figure 3 shows that α-K$_2$ZnGeO$_4$ does not follow one of these simple three patterns:

— Each tetrahedron undergoes rotation along [001] and [010].

— The periodicity of the pattern of rotation is greater than that of the C9 unit cell.

— The distortion of the framework is due to tetrahedra rotations but also to slight displacements of centers of the tetrahedra and of the K$^+$ cations.

— The tetrahedra are not perfectly regular.

In a C9 cell built with regular ZnO$_4$ (Zn–O = 1.95 Å) and GeO$_4$ (Ge–O = 1.77 Å) tetrahedra, Zn, Ge, and O atoms are lined up on the large diagonal of the cube. The Zn–Ge

TABLE 5
Coordination Polyhedra and Bond Angles in α-K_2ZnGeO_4

Tetrahedra ZnO_4 (Å)				Tetrahedra GeO_4 (Å)			
Zn(1) –O(4)	1.88(2)	Zn(2) –O(6)	1.90(2)	Ge(1) –O(7)	1.71(3)	Ge(2) –O(4)	1.73(2)
–O(3)	1.95(2)	–O(2)	1.91(2)	–O(1)	1.77(2)	–O(2)	1.76(2)
–O(5)	1.95(2)	–O(7)	1.97(2)	–O(5)	1.79(2)	–O(3)	1.77(2)
–O(1)	2.03(3)	–O(8)	1.97(2)	–O(8)	1.82(2)	–O(6)	1.80(2)
⟨m⟩	1.95	⟨m⟩	1.94	⟨m⟩	1.77	⟨m⟩	1.77

Polyhedra K–O (Å)							
K(1) –O(8)	2.51(3)	K(2) –O(4)	2.60(2)	K(3) –O(5)	2.78(3)	K(4) –O(1)	2.69(3)
–O(5)	2.66(2)	–O(6)	2.63(3)	–O(8)	2.79(3)	–O(7)	2.75(3)
–O(6)	2.75(3)	–O(7)	2.70(3)	–O(2)	2.84(3)	–O(2)	2.82(2)
–O(3)	2.77(3)	–O(5)	2.84(3)	–O(1)	2.94(2)	–O(6)	2.89(3)
–O(4)	2.85(3)	–O(3)	3.03(3)	–O(3)	3.00(3)	–O(4)	2.97(3)
–O(1)	3.32(3)	–O(2)	3.27(3)	–O(1)	3.13(2)	–O(2)	3.12(2)
–O(3)	3.35(3)	....		–O(7)	3.17(3)	–O(7)	3.30(2)
....		–O(6)	3.47(3)	–O(8)	3.29(3)	–O(8)	3.35(3)
–O(5)	3.54(2)	–O(4)	3.52(2)	....		....	
				–O(4)	3.59(3)	–O(3)	3.45(3)

Bond angle (deg)							
O–Zn–O				O–Ge–O			
O(1)–Zn(1)–O(5)	102(2)	O(2)–Zn(2)–O(8)	103(2)	O(7)–Ge(1)–O(8)	108(2)	O(4)–Ge(2)–O(6)	103(2)
O(3)–Zn(1)–O(5)	108(2)	O(7)–Zn(2)–O(8)	105(2)	O(5)–Ge(1)–O(8)	108(2)	O(3)–Ge(2)–O(6)	106(2)
O(1)–Zn(1)–O(3)	110(2)	O(2)–Zn(2)–O(6)	107(2)	O(1)–Ge(1)–O(8)	108(2)	O(3)–Ge(2)–O(4)	110(2)
O(4)–Zn(1)–O(5)	111(2)	O(6)–Zn(2)–O(7)	107(2)	O(1)–Ge(1)–O(7)	110(2)	O(2)–Ge(2)–O(4)	111(2)
O(1)–Zn(1)–O(4)	113(2)	O(6)–Zn(2)–O(8)	115(2)	O(1)–Ge(1)–O(5)	110(2)	O(2)–Ge(2)–O(6)	113(2)
O(3)–Zn(1)–O(4)	110(2)	O(2)–Zn(2)–O(7)	120(2)	O(5)–Ge(1)–O(7)	111(2)	O(2)–Ge(2)–O(3)	113(2)
⟨m⟩	109	⟨m⟩	109	⟨m⟩	109	⟨m⟩	109

Zn–O–Ge	
Zn(1)–O(1)–Ge(1)	136(3)
Zn(2)–O(2)–Ge(2)	137(3)
Zn(1)–O(3)–Ge(2)	139(3)
Zn(1)–O(4)–Ge(2)	138(3)
Zn(1)–O(5)–Ge(1)	134(3)
Zn(2)–O(6)–Ge(2)	129(2)
Zn(2)–O(7)–Ge(1)	129(2)
Zn(2)–O(8)–Ge(1)	130(2)
⟨m⟩	134

distance is equal to a quarter of this diagonal. So the ideal K_2ZnGeO_4 cell parameter should be $(1.77 \pm 1.95) \times 4/\sqrt{3} = 8.59$ Å. To compare with the real structure, we need pseudocubic cell parameters:

$$a_c = a_0/\sqrt{2} = 7.8581 \text{ Å}, \quad b_c = 2 \times b_0/\sqrt{2} = 7.8304 \text{ Å},$$

$$c_c = c_0/2 = 7.9315 \text{ Å},$$

giving a volume of 488.1 Å^3. The distortions lead to a cell parameter collapse of 8.5% for a, 8.8% for b, and 7.7% for c, that is, 23% for the volume.

The consequence of this collapse is a change in the cavities formed around potassium atoms. Figure 4 shows the potassium cavity in ideal (a) and distorted (b) surroundings. All K–O distances are equivalent in ideal form, but become strongly different in the distorted form. Some oxygen atoms are coming close to the potassium and some are going so far that they are getting out of the coordination polyhedra. A gap of about 0.2 Å in the K–O distance shows the limit of the polyhedra. Maximal distances are about 3.3 Å. The number of oxygens around the potassium varies from 6 to 9.

β-K_2ZnGeO_4

Like α-K_2ZnGeO_4, β-K_2ZnGeO_4 results from a bending of the ideal pattern. In this case the difference between ideal and real forms can be observed only on oxygen atoms.
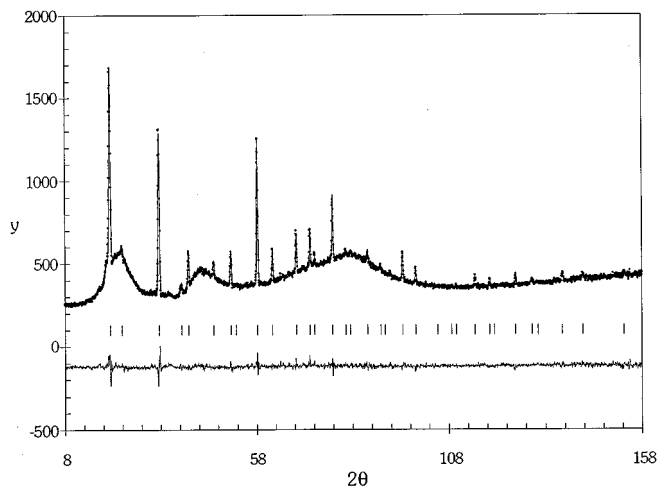
FIG. 2. Observed and calculated neutron powder diffraction patterns and difference plot of β-K$_2$ZnGeO$_4$.

The refinement leads to Zn–O and Ge–O distances and Zn–O–Ge angles consistent with values observed on compounds containing ZnO$_4$ and GeO$_4$ tetrahedra, but the oxygen position remains relatively ambiguous. The oxygen atom is distributed out of the Zn–Ge line, on six equivalent positions placed on a circle of 0.7-Å radius. The circle plane is perpendicular to the Zn–Ge line.

The β-K$_2$ZnGeO$_4$ structure can be considered as a space or time average of six equiprobable sets. Figure 5 is a (111) projection of one of these sets. The other sets are represented by the black points on the circles.

Each set follows a symmetry lower than $F\bar{4}3m$, and can be described with $I\bar{4}$ symmetry. A tetragonal cell is obtained from the cubic $C9$ cell by the transformation matrix

$$\begin{bmatrix} \frac{1}{2} & \frac{1}{2} & 0 \\ \frac{1}{2} & -\frac{1}{2} & 0 \\ 0 & 0 & 1 \end{bmatrix}.$$

The tetragonal cell parameters are $a_q = a_c/\sqrt{2} = 5.6748$ Å and $c_q = c_c = 8.0254$ Å.

TABLE 6
Refinement Details for β-K$_2$ZnGeO$_4$

Number of refined parameters	17
Independent reflections	41
R_p	1.92%
R_{wp}	2.52%
R_{exp}	2.23%
R_B	7.26%
R_F	9.39%
χ^2	1.28

TABLE 7
Crystal Data for β-K$_2$ZnGeO$_4$

Space group	$F\bar{4}3m$
Z	4
F.W.	280.16 g·mol^{-1}
a	8.0254(5) Å
V	516.9(1) Å^3
d_{calc}	3.60 g·cm^{-3}

Table 9 lists atomic coordinates in the $I\bar{4}$ space group for one set. Coordination polyhedra and bond angles are reported in Table 10. Figure 6 is a (001) projection of one set of K$_2$ZnGeO$_4$. Comparison of Figs. 3 and 6 shows that each set can be obtained from the ideal form by tetrahedral rotations following pattern I described by O'Keeffe and Hyde (8). φ, the rotation angle, is given by the relation $\tan \varphi = x/y$. φ is equal to 23.6° in β-K$_2$ZnGeO$_4$.

The consequence of these rotations is a change in the oxygen polyhedra around potassium atoms. K(1) is placed in a very open 4-coordinated polyhedron, which may explain its high Debye–Waller parameter. K(2) is placed in an 8-coordinated polyhedron.

DISCUSSION

Several compounds with the general formulas $A_2^I B^{II} X^{IV} O_4$ and $A_2^I B^{III} X^{III} O_4$, where A = Li$^+$, Na$^+$, K$^+$, Rb$^+$, Cs$^+$; B = Zn^{2+}, Mg^{2+}, Cd^{2+}, Fe^{3+}, Co^{3+}; X = Ge^{4+}, Ti^{4+}, Ga^{3+}, Al^{3+}, have been reported to have stuffed cristobalite structure (1, 9–20). All structures of these compounds stem from ideal cristobalite by tetrahedral tilt systems. A raw description based on three simple rotation patterns has been given by O'Keeffe and Hyde. This model is not sufficient to describe the complicated distortion mode of some compounds like K$_2$ZnGeO$_4$. Indeed, it has been shown that the monovalent cation radius has a great influence on the rotation pattern (1, 21).

In the case of α-K$_2$ZnGeO$_4$, our neutron diffraction data allowed differentiation between Zn and Ge atoms, showing ordered and alternating ZnO$_4$ and GeO$_4$ tetrahedra. This arrangement leads to the polar space group $Pca2_1$. The transition from this space group to the acentric nonpolar

TABLE 8
Positional and Debye–Waller Parameters for β-K$_2$ZnGeO$_4$

Atom	x/a	y/b	z/c	B (Å^2)	Position	Occupancy
Ge	0	0	0	4.7(2)	4a	1
Zn	1/4	1/4	1/4	3.2(3)	4c	1
K(1)	1/2	1/2	1/2	10.4(9)	4b	1
K(2)	3/4	3/4	3/4	5.9(5)	4d	1
O	0.1893(10)	0.0742(19)	0.1041(21)	4.7(2)	96i	1/6

a

b

FIG. 3. K_2ZnGeO_4 double cell in cubic system: (a) ideal form, (b) distorted form.
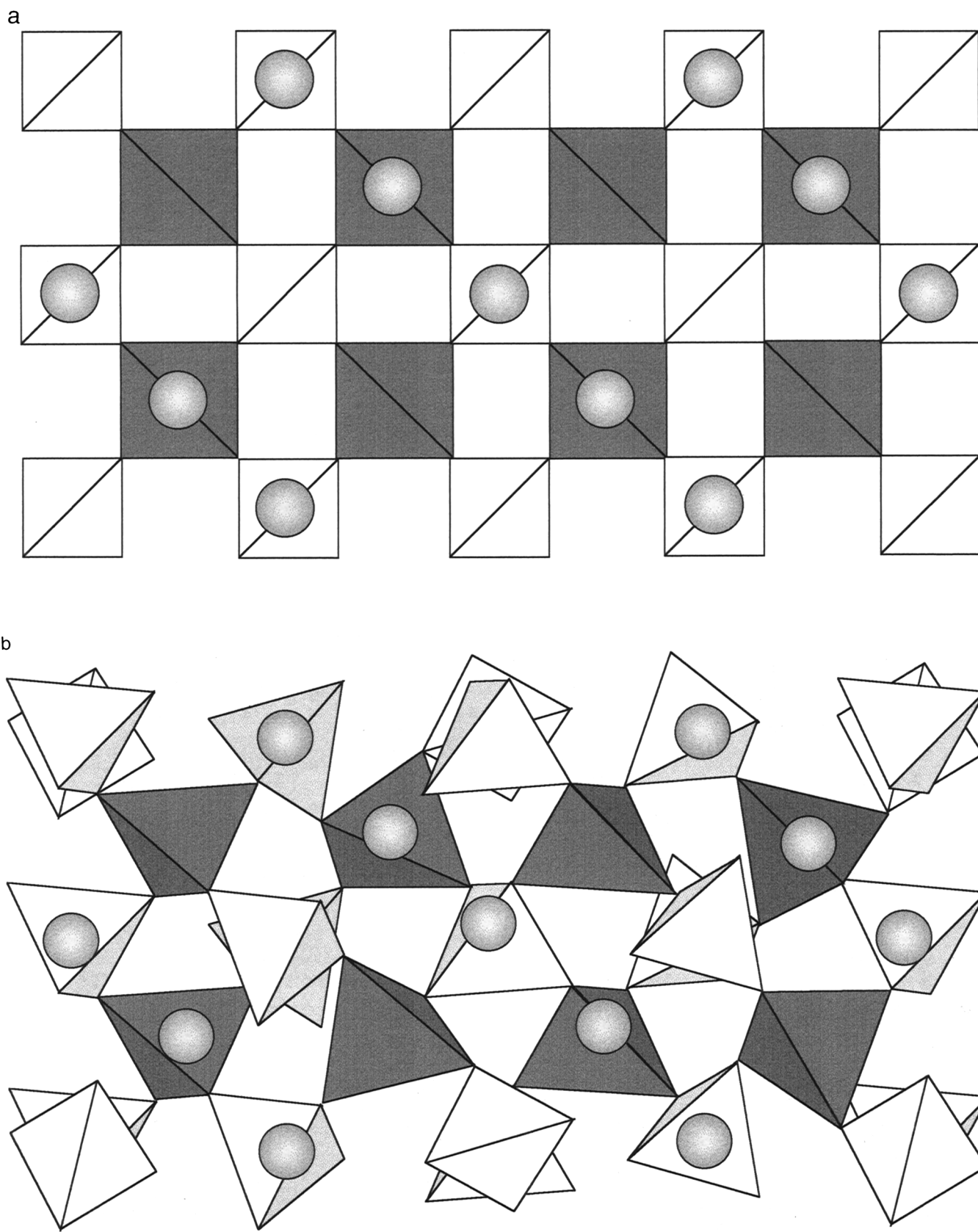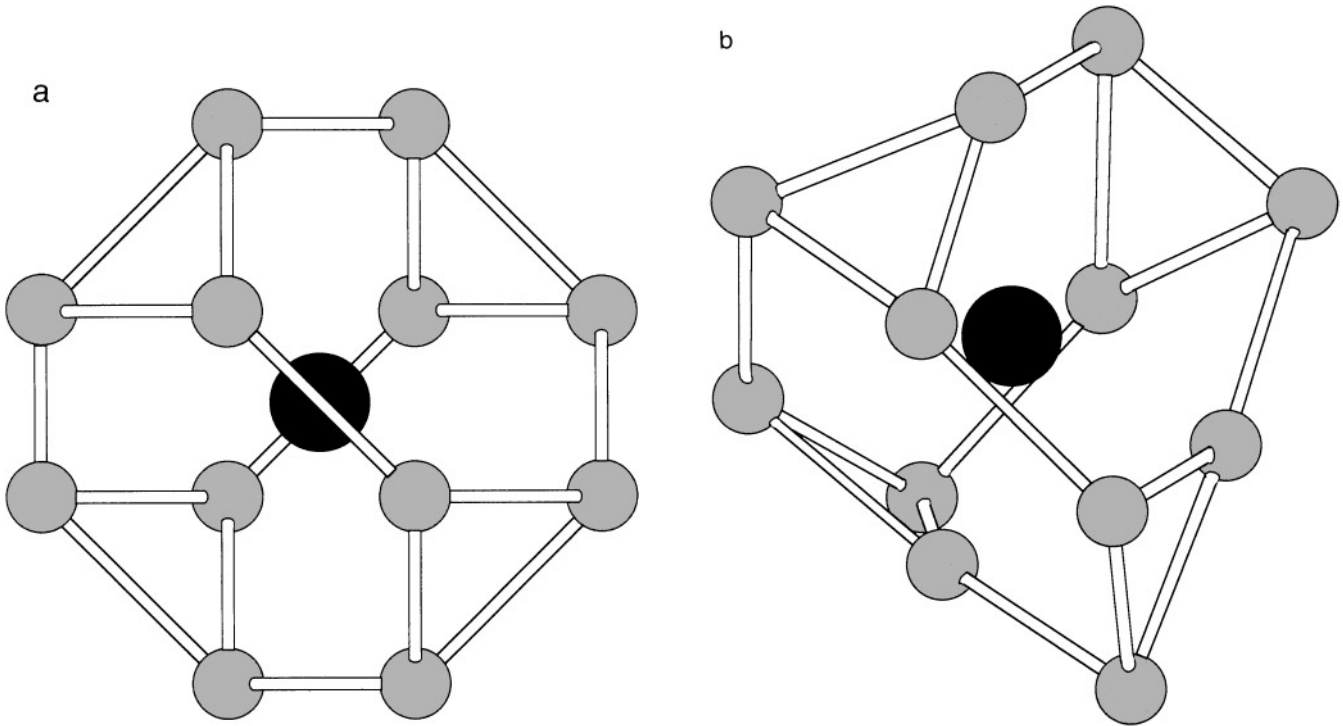
FIG. 4. K cavity of K$_2$ZnGeO$_4$: (a) ideal form, (b) α-form.

$F\bar{4}3m$ space group is potentially ferroelectric. This behavior has been evidenced (1, 3, 22) by a maximum in the thermal variation of the dielectric permittivity (ε) at the phase transition, also called Curie point. The discontinuity

observed at this point in the curve, $1/\varepsilon = f(T)$, implies a first-order transition. A detailed analysis of the ferroelectric and ferroelastic behavior of K$_2$ZnGeO$_4$ will be published later.

In the case of β-K$_2$ZnGeO$_4$, our neutron diffraction data allowed us to show a delocalization of oxygen atoms. The structure is a six-set average one, each set having a lower symmetry than the average form. The diffraction data do not tell us if it is a time or space average. Such a problem has been observed in β-cristobalite form of SiO$_2$ (23) and AlPO$_4$ (24) compounds. Some recent experiments have been performed to answer the question linked to the nature of the disorder.

Schmahl *et al.* (25) performed high-resolution neutron diffraction experiments on β-SiO$_2$. No line broadening
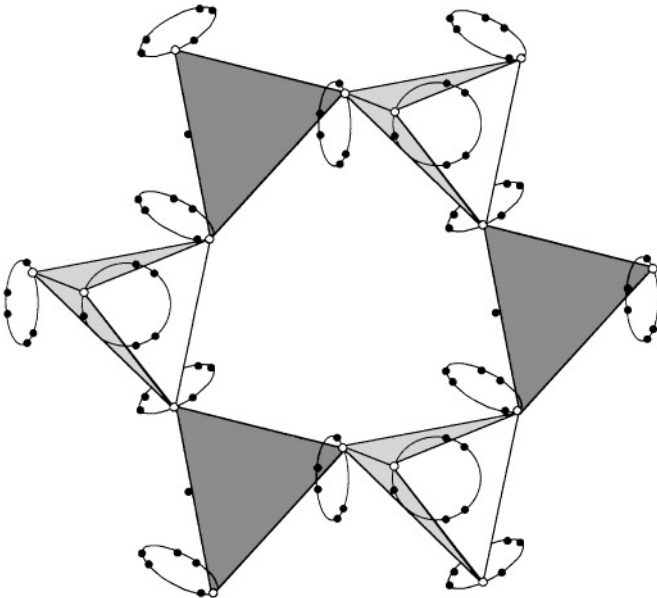
FIG. 5. β-K$_2$ZnGeO$_4$, projection (111).

TABLE 9
Positional Parameters in $I\bar{4}$ Space Group for One β-K$_2$ZnGeO$_4$ Set

Atom	x/a	y/b	z/c	Position	Occupancy
Ge	0	0	0	2a	1
Zn	0	1/2	1/4	2c	1
K(1)	0	0	1/2	2b	1
K(2)	0	1/2	3/4	2d	1
O	0.1151	0.2635	0.1041	8g	1

TABLE 10
Coordination Polyhedra and Bond Angles in β-K$_2$ZnGeO$_4$

ZnO$_4$ and GeO$_4$ tetrahedra (Å)			
Zn–O	1.90(2) ×4	Ge–O	1.83(2) ×4

Polyhedra K–O (Å)			
K(1)–O	2.70(1) ×4	K(2)–O	2.89(2) ×4
	3.57(2) ×4		3.21(2) ×4
	3.83(2) ×4		3.97(2) ×4

Bond angle (deg)			
O–Zn–O		O–Ge–O	Zn–O–Ge
112(2) ×4		102(2) ×4	137(2)
104(2) ×2		125(2) ×2	
$\langle m \rangle$ 109		$\langle m \rangle$ 110	

corresponding to tetragonal microdomains was observed, in agreement with our observations on K$_2$ZnGeO$_4$.

Hatch and Ghose (26) suggested that β-SiO$_2$ is a dynamic average of microscopic domains of the α form with fluctuat-ing domain walls. This model is based on a theoretical analysis of the symmetry of the transition between α and β forms of SiO$_2$. NMR results of ^{29}Si and ^{17}O elements have been interpreted by this model (27).
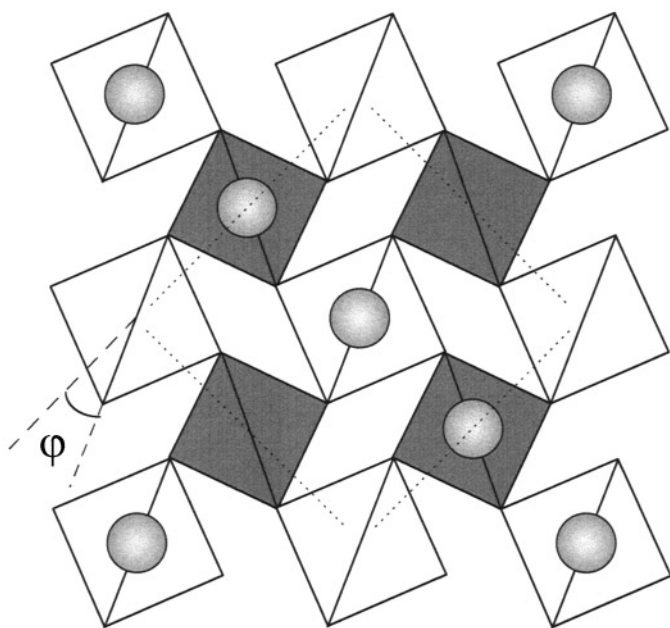
Swainson and Dove (28) made inelastic neutron scatter-ing and confirmed the existence of the important number of low-frequency floppy modes called RUMs (rigid unit modes) in β-SiO$_2$. They showed with infrared experiments that β-SiO$_2$ is a true dynamically disordered phase, as tacitly assumed in the RUM model, and does not contain static or dynamic domains of the α form. Molecular dynam-ics simulations show that the disorder is better described by a random precession of the Si–O bonds rather than the hopping of O atoms between specific sites.

FIG. 6. One set of β-K$_2$ZnGeO$_4$, projection (001).

REFERENCES

1. C. Colbeau-Justin, Ph.D. thesis, Université Pierre et Marie Curie, Paris, 1996.
2. C. Colbeau-Justin, A. Elfakir, and M. Quarton, *Powder Diffraction* **9,** 146 (1994).
3. C. Colbeau-Justin, A. Elfakir, and M. Quarton, *Ferroelectrics* **185,** 157 (1995).
4. C. Colbeau-Justin, G. Wallez, A. Elfakir, and M. Quarton, *Powder Diffraction* (1997), in press.
5. J. Grins and D. Louër, *J. Solid State Chem.* **87,** 114 (1990).
6. J. Rodriguez-Carvajal, *in* "Collected Abstracts of Powder Diffraction Meeting," Toulouse, France, p. 127 (1990).
7. R. W. G. Wyckoff, *Am. J. Sci.* **9,** 448 (1925).
8. M. O'Keeffe and B. G. Hyde, *Acta Crystallogr. Sect. B* **32,** 2923 (1976).
9. P. Bertaut and P. Blum, *C. R. Acad. Sci. Paris* **239,** 429 (1954).
10. M. Marezio, *Acta Crystallogr.* **19,** 396 (1965).
11. M. Marezio, *Acta Crystallogr.* **18,** 481 (1965).
12. E. Vielhaber and R. Hoppe, *Z. Anorg. Allg. Chem.* **369,** 14 (1969).
13. C. Delmas, C. Fouassier, and P. Hagenmuller, *J. Solid State Chem.* **13,** 165 (1975).
14. Z. Tomkowicz and A. Szytula, *J. Phys. Chem. Solids* **38,** 1117 (1977).
15. A. Maazaz and C. Delmas, *Solid State Ionics* **6,** 261 (1982).
16. C. Delmas, A. Maazaz, and P. Hagenmuller, *Solid State Ionics* **9/10,** 83 (1983).
17. S. Frostäng, J. Grins, D. Louër, and P.-E. Werner, *Solid State Ionics* **31,** 131 (1988).
18. L. M. Torres-Martinez and A. R. West, *J. Mater. Sci. Lett.* **7,** 821 (1988).
19. S. Frostäng and P.-E. Werner, *Mater. Res. Bull.* **24,** 833 (1989).
20. B. Maksimov, R. Tamazyan, M. I. Sirota, S. Frostäng, J. Grins, and M. Nygren, *J. Solid State Chem.* **86,** 64 (1990).
21. C. Colbeau-Justin, G. Wallez, A. Elfakir, and M. Quarton, to be published (1997).
22. C. Colbeau-Justin, A. Elfakir, and M. Quarton, *in* "Proceedings, XXIèmes Journées d'Etude des Equilibres entre Phases," Rouen, France, 1995.
23. D. R. Peacor, *Z. Kristallogr.* **138,** 274 (1973).
24. A. F. Wright and A. J. Leadbetter, *Phil. Mag.* **31,** 1391 (1975).
25. W. W. Schmahl, I. P. Swainson, M. T. Dove, and A. Graeme-Barber, *Z. Kristallogr.* **201,** 125 (1992).
26. D. M. Hatch and S. Ghose, *Phys. Chem. Miner.* **17,** 554 (1991).
27. D. M. Hatch, S. Ghose, and J. Bjorkstam, *Phys. Chem. Miner.* **21,** 67 (1994).
28. I. P. Swainson and M. T. Dove, *Phys. Rev. Lett.* **71,** 193 (1993).